Design and synthesis of squaramide-based MOFs as efficient MOF-supported hydrogen-bonding organocatalysts†

Xiaoping Zhang,‡[ab] Zhenjie Zhang,‡[a] Jake Boissonnault[a] and Seth M. Cohen*[a]

Herein, we utilize a new, squaramide-based ligand, combined with a postsynthetic exchange (PSE) synthetic approach to prepare a series of Cu(II)–squaramide MOFs that are active catalysts for the Friedel–Crafts reaction.

Among various organocatalysts, those based on the thiourea core are broadly utilized in the field of H-bond donor catalysis.[1] Recently, bifunctional squaramide moieties have emerged as powerful hydrogen-bonding groups for Lewis acid catalysis.[2–8] Squaramides are four-membered ring systems, which are derived from squaric acid and possess hydrogen-bond accepting and donating functionality through their carbonyl and N–H groups, respectively. The squaramide functionality possesses features such as ditopic binding, structural rigidity, high N–H acidity, and ease of preparation.[9] Squaramide compounds have been shown to be competent for biomimetic transport,[5,10,11] molecular recognition,[12] ion sensing,[13,14] and organocatalysis.[15,16] The high propensity for hydrogen-bonding is driven *via* a concomitant increase in aromaticity on the squaramide ring.[17] Although the increased acidity of squaramides can be useful in hydrogen-bond donating organocatalysis, the strong hydrogen-bonding also drives self-association/aggregation of squaramides that impedes catalysis.[18] To prevent self-association and enhance the catalytic performance of squaramides, one strategy is to immobilize these groups within porous materials such as metal–organic frameworks (MOFs).[19,20]

MOFs are a class of porous, crystalline materials composed of inorganic nodes and organic linkers. They have uniform 3-dimensional structures of high surface area, large pore sizes, low density, and have potential applications in gas sorption,[21,22] molecular recognition,[23] proton conductivity,[24] and organocatalysis.[25–29] Along with their modular synthesis and tunable porosity, MOFs constitute attractive candidates as platforms for heterogeneous catalysis.

To incorporate squaramide catalysts into MOFs, a feasible design approach is to employ squaramide compounds as ligand struts for MOFs. Hupp, Farha, and Mirkin developed a mixed-ligand MOF catalyst, UiO-67-Squar/bpdc,[20] which was constructed using a combination of unfunctionalized and squaramide-appended biphenyl dicarboxylate (bpdc) ligands. In this system, the squaramide group was attached as a 'dangling' substituent off of the bpdc ligand framework. The percentage of squaramide ligand incorporation was varied from 0–100%. The authors reported that MOFs with 100% squaramide ligand incorporation showed low catalytic activity, similar to those MOFs with 100% unfunctionalized bpdc ligand (*e.g.* no catalytic sites). MOFs with 50% squaramide ligand exhibited the highest catalytic activity, which was attributed to an optimal balance of catalytic sites and sufficient retention of MOF porosity. Herein, an alternative approach presented for squaramide-based MOF catalysts is described. A new squaramide ligand with four carboxylate ligating groups (5,5′-(3,4-dioxocylcobut-1-ene-1,2-diyl)bis(azanediyl)diisophthalic acid, H₄dbda, Fig. 1) has been designed and synthesized. Using H₄dbda, we developed a stable Cu-MOF, [Cu₂(dbda)(CH₃OH)₂] (**Cu(dbda)**), through a postsynthetic exchange (PSE) reaction from its Zn(II) analogue, [Zn₂(dbda)(H₂O)₂] (**Zn(dbda)**). The Friedel–Crafts reaction, a prototypical reaction for hydrogen-bonding organocatalyst,[30–34] was selected to evaluate the catalytic performance of these MOFs (Fig. 1). **Cu(dbda)** demonstrated high catalytic efficiency for the Friedel–Crafts reaction between indole and substituted β-nitrostyrenes while **Zn(dbda)** was not a catalyst due to its poor stability. The **Cu(dbda)** system allows for 100% incorporation of the H₄dbda squaramide ligand without a significant loss of MOF porosity.

The H₄dbda ligand was synthesized using a modified literature procedure.[35] Both ¹H NMR and MS data confirmed the composition of the ligand (Fig. S1 and S2, ESI†). Combining H₄dbda and

a Department of Chemistry and Biochemistry, University of California, San Diego, La Jolla, California 92093, USA. E-mail: scohen@ucsd.edu

b Department of Chemistry, Key Laboratory of Advanced Energy Materials Chemistry (MOE), Collaborative Innovation Center of Chemical Science and Engineering, Nankai University, Tianjin 300071, P. R. China
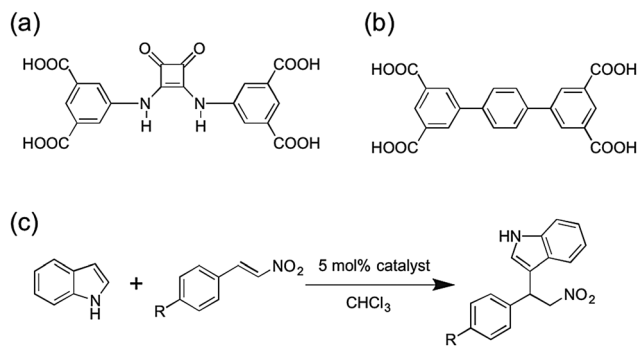
‡ These authors contributed equally.

Fig. 1 (a) Structure of the H$_4$dbda ligand. (b) Structure of H$_4$tptc ligand. (c) Friedel–Crafts reaction between indole and substituted β-nitrostyrenes.

Zn(NO$_3$)$_2$ in a mixture of DMF and EtOH at 80 °C for 24 h afforded pale-yellow crystals of **Zn(dbda)**. Single-crystal X-ray diffraction (XRD) structure determination revealed that **Zn(dbda)** crystallized in the $R\bar{3}m$ space group with unit cell parameters $a = b = 18.8687(9)$ Å, $c = 38.3555(17)$ Å, $\alpha = \beta = 90°$, $\gamma = 120°$ (Table S1, ESI†). As shown in Fig. 2, **Zn(dbda)** is built by [Zn$_2$(COO)$_4$] paddlewheel secondary building units (SBUs). The 1,3-benzenedicarboxylate (1,3-bdc) moieties in dbda^{4-} are linked by [Zn$_2$(COO)$_4$] SBUs to form a 2-dimensional Kagomé lattice that are connected via the squaramide core to form an overall 3-dimensional framework with nbo topology (Fig. S3 and S4, ESI†). There are large channels with approximate dimensions of 13×5 Å along the crystallographic c-axis. N$_2$ sorption of **Zn(dbda)** showed essentially no uptake (Fig. 3), which is attributed to a loss of **Zn(dbda)** crystallinity upon thermal activation (60 °C, 10 h) as evidenced by powder X-ray diffraction (PXRD, Fig. S5, ESI†). **Zn(dbda)** was found to be stable in common organic solvents such as CHCl$_3$ for 24 h at room temperature, but not stable in water (Fig. S6 and S7, ESI†). Despite these stability limitations, the catalytic performance of **Zn(dbda)** in the Friedel–Crafts reaction was examined. Indole (0.15 mmol) and β-nitrostyrene (0.1 mmol) were chosen as test substrates, and the reaction was performed at 50 °C in CHCl$_3$ with 5 mol% loading of the **Zn(dbda)** catalyst (based on an empirical formula of Zn$_4$(dbda)$_2$(H$_2$O)$_4$); however, no products were observed after 24 h (Fig. S8, ESI†). PXRD of **Zn(dbda)** after 24 h revealed that the MOF had lost crystallinity under the reaction conditions (Fig. S9, ESI†).

Literature reports suggest that [Zn$_2$(COO)$_4$] SBUs may possess low chemical stability.[36] However, there are reports of Zn(II)

Fig. 2 Coordination environment of **Zn(dbda)** (left). Packing of **Zn(dbda)** along the crystallographic c-axis (right). Color code: O, red; N, blue; Zn, cyan; C, gray.
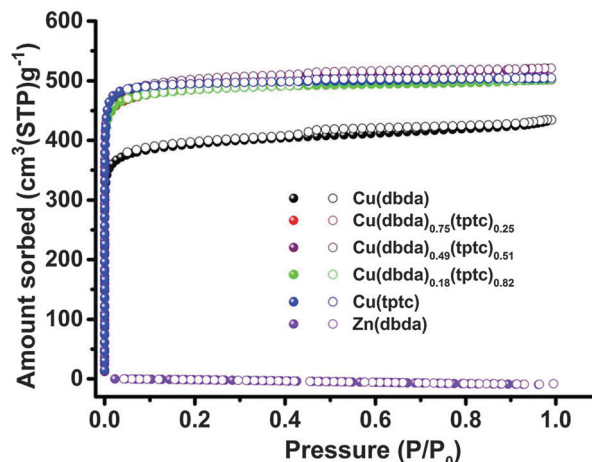

Fig. 3 N$_2$ gas sorption of **Cu(dbda)$_x$(tptc)$_{1-x}$** (x = 1, 0.75, 0.49, 0.18, 0). Adsorption and desorption branches are shown with filled and empty symbols, respectively.

SBUs that can undergo PSE with Cu(II) cations and the resulting Cu(II)-based SBUs showing greater chemical stability.[37] PSE of **Zn(dbda)** with Cu(NO$_3$)$_2$ produced a new compound **Cu(dbda)** (Fig. S10, ESI†); attempts to prepare **Cu(dbda)** directly from H$_4$dbda and various Cu salts were unsuccessful under a variety of reaction conditions. Both EDX (~99% Cu) and ICP-OES (~99% Cu) showed that the Zn(II) ions were essentially completely replaced by Cu(II) by this PSE process (Fig. S11 and Table S2, ESI†). XRD of **Cu(dbda)** revealed that **Cu(dbda)** exhibited the same structure as **Zn(dbda)**, with only slight differences in cell parameters: $a = b = 18.2623(6)$ Å, $c = 39.6543(13)$ Å. **Cu(dbda)** possesses a slightly smaller unit cell ($V = 11453.3(7)$ Å^3) than **Zn(dbda)** ($V = 11826.1(10)$ Å^3) (Table S3, ESI†) due to the shorter Cu–O bonds. For **Zn(dbda)**, the average distance of Zn–O (carboxylate) bonds is 2.036 Å, while for **Cu(dbda)**, the average Cu–O (carboxylate) distance is 1.947 Å. Moreover, the metal–metal distance in the paddlewheel SBUs decreased from 2.999 Å (Zn–Zn) to 2.629 Å (Cu–Cu). The permanent porosity of **Cu(dbda)** was measured by N$_2$ absorption at 77 K, which showed a typical type I isotherm,[38] giving a BET surface area of 1516 ± 66 m^2 g^{-1} and a total pore volume of 0.662 cm^3 g^{-1} (Fig. 3). The PXRD pattern of **Cu(dbda)** remains intact upon immersion in organic solvents for 90 h, suggesting improved stability consistent with the gas sorption data; however, **Cu(dbda)** was unstable in water (Fig. S12 and S13, ESI†).

The model reaction between indole (0.15 mmol) and β-nitrostyrene (0.10 mmol, Fig. 1) was examined with 5 mol% loading of **Cu(dbda)** (based on an empirical formula of Cu$_4$(dbda)$_2$-(CH$_3$OH)$_4$) as a catalyst. Under identical conditions to those reported for UiO-67-Squar/bpdc (CD$_2$Cl$_2$, 25 °C, 24 h), **Cu(dbda)** gave a yield of only 32%, compared to 78% for UiO-67-Squar/bpdc.[20] Therefore, reaction conditions were optimized for **Cu(dbda)** including the use of different solvents (toluene, CH$_3$CN, CHCl$_3$) and temperatures (25, 35, and 50 °C) (Table S4 and Fig. S14, ESI†). It was found that CHCl$_3$ gave the best results, and activity could be increased with increasing temperature from ~60% (25 °C), to ~78% (35 °C), to >99% (50 °C). Control reactions

either without catalyst or with free H_4dbda ligand (not as part of a MOF) were also performed under the same optimized reaction conditions. Without catalyst, no product was observed. The catalytic activity of free H_4dbda was much lower than the MOF, giving a yield of only 33% after 24 h (Fig. S15, ESI†). The improved activity of **Cu(dbda)** suggests that the MOF prevents squaramide self-aggregation, which likely causes the sluggish activity of the free H_4dbda ligand. A time-dependent study was performed from 30 min to 24 h (Fig. S16, ESI†). The conversion of β-nitrostyrene was ~60% (turnover frequency, TOF = 3.0 × 10^{-3} s^{-1}) after 1 h, with 95% conversion after 8 h (TOF = 6.6 × 10^{-4} s^{-1}), and complete consumption of the starting material after 24 h.

An advantage of heterogeneous catalysts is reusability, which was also investigated for **Cu(dbda)**. Only a small decrease in activity (from >99% to ~96%) was observed after 5 runs (Fig. S17, ESI†). Characterization of **Cu(dbda)** after the 5th run showed the catalyst retained its crystallinity, with the PXRD pattern of the recycled **Cu(dbda)** in good agreement with the calculated patterns (Fig. S18, ESI†). A test was performed to confirm the heterogeneity of the catalysts (and rule out soluble species) by removing the MOF catalyst by filtration after 30 min (at which time the yield was ~22%). The filtrate was then re-analyzed after a total of 24 h showing no formation of new product and indicating that the catalyst is heterogeneous and there is no leaching of a catalytic species into solution (Fig. S16, ESI†).[20] The substrate scope for various substituted-nitrostyrene derivatives was also examined to assess the utility of **Cu(dbda)** (Fig. S19, ESI†). Good to excellent yields, ranging from ~61% for 4-nitro-β-nitrostyrene (poor solubility in $CHCl_3$) to 97% for 4-chloro-β-nitrostyrene, were obtained (Table 1). Overall, these results show that **Cu(dbda)** is an efficient, recyclable, heterogeneous catalyst for the Friedel–Crafts reaction.

To further investigate the catalytic activity of **Cu(dbda)**, a series of isostructural MOF catalysts, $[Cu_2(dbda)_x(tptc)_{1-x}(CH_3OH)_2]$ (**Cu(dbda)$_x$(tptc)$_{1-x}$**, x = 0.75, 0.49, 0.18, 0; H_4tptc = p-terphenyl-3,5,3″,5″-tetracarboxylic acid, Fig. 1), were prepared via a mixed-ligand strategy; the single-crystal structure of **Cu(tptc)** was previously reported in 2006.[39] The structures of the two tetracarboxylic ligands (H_4dbda and H_4tptc) are very similar, both using square-planar 4-connected nodes with the distance between 4 and 4′ carbon atoms in H_4dbda of 11.57 Å versus 11.38 Å in H_4tptc. The synthesis of **Cu(dbda)$_x$(tptc)$_{1-x}$** (x = 0.75, 0.49, 0.18) was achieved via a PSE approach using **Zn(dbda)$_x$(tptc)$_{1-x}$** MOFs as precursors. Both EDX and ICP-OES results (Table S2 and Fig. S20–S23, ESI†) showed the metal content of Cu(II) in all of the **Cu(dbda)$_x$(tptc)$_{1-x}$** (x = 0.75, 0.49, 0.18, 0) was >92%, thus indicating near complete PSE. The PXRD patterns of the mixed-ligand MOFs **Cu(dbda)$_x$(tptc)$_{1-x}$** were all in good agreement with calculated patterns (Fig. S24, ESI†). The ratio of $dbda^{4-}$ and $tptc^{4-}$ in **Cu(dbda)$_x$(tptc)$_{1-x}$** (x = 0.75, 0.49, 0.18) determined by ^{1}H NMR (Fig. S25, ESI†) were very close to the expected values (0.75, 0.50, and 0.25 based on the ratio of starting materials). In addition, a direct solvothermal synthesis was examined for the preparation of **Cu(dbda)$_x$(tptc)$_{1-x}$**.[39] However, the loading of $dbda^{4-}$ through solvothermal methods was much lower than

Table 1 Friedel–Crafts reaction between indole and β-nitrostyrenes to produce 3-(2-nitro-1-phenylethyl)-1H-indoles

Entry	R^a	Catalyst	Temp. (°C)	Time (h)	Yield (%)
1	H	None	50	24	0
2	H	H_4dbda^a	50	24	32
3	H	$Cu(NO_3)_2$^{b}	50	24	28
4	H	**Zn(dbda)**	50	24	0
5	H	**Cu(dbda)**	25	24	60
6	H	**Cu(dbda)**	35	24	78
7	H	**Cu(dbda)**	50	1	60
8	H	**Cu(dbda)**	50	8	95
9	H	**Cu(dbda)**	50	24	>99
10	Cl	**Cu(dbda)**	50	24	97
11	F	**Cu(dbda)**	50	24	91
12	Br	**Cu(dbda)**	50	24	92
13	CH_3	**Cu(dbda)**	50	24	90
14	OCH_3	**Cu(dbda)**	50	24	74
15	NO_2	**Cu(dbda)**	50	24	61
16	H	**Cu(dbda)$_{0.75}$(tptc)$_{0.25}$**	50	24	99
17	H	**Cu(dbda)$_{0.49}$(tptc)$_{0.51}$**	50	24	95
18	H	UiO-67-Squar/bpdc^c	50	24	95
19	H	UiO-67-Urea/bpdc^c	50	24	79
20	H	**Cu(dbda)$_{0.18}$(tptc)$_{0.82}$**	50	24	88
21	H	**Cu(tptc)**	50	24	38

Conditions: indole (0.15 mmol), β-nitrostyrenes (0.10 mmol), and catalyst (5 mol%) in $CHCl_3$ (1 mL). Yields monitored by ^{1}H NMR. See ESI for details. ^{a} Catalyst loading was 10 mol%. ^{b} Catalyst loading was 20 mol%. ^{c} Conditions: indole (0.02 mmol), β-nitrostyrene (0.014 mmol), and catalyst (10 mol%) in toluene (0.7 mL), see ref. 20 for details.

the ratio used in the synthesis, with initial ratios of $dbda^{4-}$ of 0.50 and 0.25 giving incorporation of only x = 0.31 and 0.12, respectively. Moreover, **Cu(dbda)** could not be obtained using solvothermal methods (Fig. S26 and S27, ESI†). The permanent porosity of **Cu(dbda)$_x$(tptc)$_{1-x}$** were also evaluated by N_2 sorption isotherms at 77 K, giving the expected type-I isotherms (Fig. 3). The BET surface areas of **Cu(dbda)$_x$(tptc)$_{1-x}$** (x = 0.75, 0.49, 0.18) were 1884 ± 61 m^2 g^{-1}, 1946 ± 124 m^2 g^{-1}, and 1887 ± 45 m^2 g^{-1}, respectively, with total pore volumes of **Cu(dbda)$_x$(tptc)$_{1-x}$** (x = 0.75, 0.49, 0.18) of 0.775 cm^3 g^{-1}, 0.803 cm^3 g^{-1}, and 0.775 cm^3 g^{-1}, respectively. These results show that the porosity of the **Cu(dbda)$_x$(tptc)$_{1-x}$** fall in the expected range between those of the single-ligand MOFs, **Cu(dbda)** (1516 m^2 g^{-1}) and **Cu(tptc)** (1942 m^2 g^{-1}).

Cu(dbda)$_x$(tptc)$_{1-x}$ was employed as catalyst for the Friedel–Crafts reaction between indole (0.15 mmol) and β-nitrostyrene (0.1 mmol), carried out at 50 °C in $CHCl_3$ for 24 h (5 mol% loading, based on the empirical formula $Cu_4(dbda)_{2x}(tptc)_{2-2x}(H_2O)_4$, x = 0.75, 0.49, 0.18). Using **Cu(tptc)** (5 mol% loading, no squaramide sites) as a catalyst gave a low yield of ~39% (Fig. S28, ESI†); the residual activity may arise from the Lewis acid Cu(II) sites, as Cu(II)-complexes have been reported to show catalytic activity for the Friedel–Crafts reaction.[40] Consistent with this observation, $Cu(NO_3)_2$, gave a 28% conversion under the same reaction conditions. In contrast, for **Cu(dbda)$_x$(tptc)$_{1-x}$** (x = 1, 0.75, 0.49, 0.18, 0), activity increased with increasing $dbda^{4-}$ content: 39% (**Cu(tptc)**), 88% (**Cu(dbda)$_{0.18}$(tptc)$_{0.82}$**), 95% (**Cu(dbda)$_{0.49}$(tptc)$_{0.51}$**), 99% (**Cu(dbda)$_{0.75}$(tptc)$_{0.25}$**), and >99% (**Cu(dbda)**), respectively. These results verify that the squaramide group is the governing catalytic functional group

in these MOFs. For a more direct comparison to the prior reports,[20] a 2.45 mol% loading of catalyst **Cu(dbda)$_{0.49}$(tptc)$_{0.51}$** achieved the same catalytic performance as the reported UiO-67-Squar/bpdc at 10 mol% loading (95% yield at 50 °C for 24 h).[20] The result further verified the high activity of the dbda^{4-}-based MOF.

Taken together, **Cu(dbda)** has features that compliment and distinguish it from the previously reported UiO-67-Squar/bpdc catalyst.[20] **Cu(dbda)** has a different MOF structure type from UiO-67-Squar/bpdc, wherein the catalytic group is part of the ligand 'backbone' rather than a dangling component. Depending on catalyst design, one can envision scenarios where one or the other functional group arrangement might be preferable. Also, in contrast to UiO-67-Squar/bpdc, **Cu(dbda)** allows for 100% functional ligand incorporation without loss of surface area. Indeed, using H$_4$tptc as a complimentary, unfunctionalized ligand the **Cu(dbda)** system is not limited with respect to the amount of squaramide ligand that can be included while maintaining a high degree of porosity and activity. Both **Cu(dbda)$_x$(tptc)$_{1-x}$** and UiO-67-Squar/bpdc catalysts show good activity under similar conditions, and hence each helps advance the ability of utilizing squaramides in MOF-based catalytic systems.

In summary, we prepared a squaramide tetracarboxylate ligand, and developed catalytic squaramide MOFs prepared *via* metal PSE from Zn(II) precursor MOFs. The Cu(II) MOFs were more stable and hence showed good catalytic performance when compared to the unstable parent Zn(II) MOF, in a Friedel–Crafts reaction of indole with β-nitrostyrenes. A series of isostructural MOFs **Cu(dbda)$_x$(tptc)$_{1-x}$** ($x = 0.75, 0.49, 0.18, 0$) showed that the catalytic performance of these MOFs increased with increasing amounts of the squaramide ligand, demonstrating that squaramide MOFs are promising MOF-supported heterogeneous organocatalysts. Our ongoing progress with squaramide MOFs are focusing on their applications in molecular recognition and ion sensing.

Notes and references

1 S. J. Connon, *Chem. – Eur. J.*, 2006, **12**, 5418–5427.
2 J. Aleman, A. Parra, H. Jiang and K. A. Jorgensen, *Chem. – Eur. J.*, 2011, **17**, 6890–6899.
3 R. I. Storer, C. Aciro and L. H. Jones, *Chem. Soc. Rev.*, 2011, **40**, 2330–2346.
4 J. P. Malerich, K. Hagihara and V. H. Rawal, *J. Am. Chem. Soc.*, 2008, **130**, 14416–14417.
5 D. Roca-Lopez, U. Uria, E. Reyes, L. Carrillo, K. A. Jorgensen, J. L. Vicario and P. Merino, *Chem. – Eur. J.*, 2016, **22**, 884–889.
6 Y. Wang, J. Pan, R. Jiang, Y. Wang and Z. Zhou, *Adv. Synth. Catal.*, 2016, **358**, 195–200.
7 H. Zhang, S. Lin and E. N. Jacobsen, *J. Am. Chem. Soc.*, 2014, **136**, 16485–16488.
8 C. H. Cheon and H. Yamamoto, *Tetrahedron Lett.*, 2009, **50**, 3555–3558.
9 P. Chauhan, S. Mahajan, U. Kaya, D. Hack and D. Enders, *Adv. Synth. Catal.*, 2015, **357**, 253–281.
10 Y. Zhu, J. P. Malerich and V. H. Rawal, *Angew. Chem., Int. Ed.*, 2010, **49**, 153–156.
11 H. Jiang, M. W. Paixao, D. Monge and K. A. Jorgensen, *J. Am. Chem. Soc.*, 2010, **132**, 2775–2783.
12 B. Soberats, L. Martinez, E. Sanna, A. Sampedro, C. Rotger and A. Costa, *Chem. – Eur. J.*, 2012, **18**, 7533–7542.
13 X. Wu, N. Busschaert, N. J. Wells, Y. B. Jiang and P. A. Gale, *J. Am. Chem. Soc.*, 2015, **137**, 1476–1484.
14 C. Gaeta, C. Talotta, P. Della Sala, L. Margarucci, A. Casapullo and P. Neri, *J. Org. Chem.*, 2014, **79**, 3704–3708.
15 B. Shan, Y. Liu, R. Shi, S. Jin, L. Li, S. Chen and Q. Shu, *RSC Adv.*, 2015, **5**, 96665–96669.
16 A. Rostami, C. J. Wei, G. Guerin and M. S. Taylor, *Angew. Chem., Int. Ed.*, 2011, **50**, 2059–2062.
17 D. Quiñonero, R. Prohens, C. Garau, A. Frontera, P. Ballester, A. Costa and P. M. Deyà, *Chem. Phys. Lett.*, 2002, **351**, 115–120.
18 A. Portell, R. Barbas, D. Braga, M. Polito, C. Puigjaner and R. Prohens, *CrystEngComm*, 2009, **11**, 52–54.
19 J. V. Alegre-Requena, E. Marqués-López, R. P. Herrera and D. D. Díaz, *CrystEngComm*, 2016, **18**, 3985–3995.
20 C. M. McGuirk, M. J. Katz, C. L. Stern, A. A. Sarjeant, J. T. Hupp, O. K. Farha and C. A. Mirkin, *J. Am. Chem. Soc.*, 2015, **137**, 919–925.
21 L. Du, Z. Lu, K. Zheng, J. Wang, X. Zheng, Y. Pan, X. You and J. Bai, *J. Am. Chem. Soc.*, 2013, **135**, 562–565.
22 J. A. Mason, J. Oktawiec, M. K. Taylor, M. R. Hudson, J. Rodriguez, J. E. Bachman, M. I. Gonzalez, A. Cervellino, A. Guagliardi, C. M. Brown, P. L. Llewellyn, N. Masciocchi and J. R. Long, *Nature*, 2015, **527**, 357–361.
23 B. Chen, S. Xiang and G. Qian, *Acc. Chem. Res.*, 2010, **43**, 1115–1124.
24 N. T. Nguyen, H. Furukawa, F. Gandara, C. A. Trickett, H. M. Jeong, K. E. Cordova and O. M. Yaghi, *J. Am. Chem. Soc.*, 2015, **137**, 15394–15397.
25 M. H. Beyzavi, R. C. Klet, S. Tussupbayev, J. Borycz, N. A. Vermeulen, C. J. Cramer, J. F. Stoddart, J. T. Hupp and O. K. Farha, *J. Am. Chem. Soc.*, 2014, **136**, 15861–15864.
26 J. Liu, L. Chen, H. Cui, J. Zhang, L. Zhang and C. Y. Su, *Chem. Soc. Rev.*, 2014, **43**, 6011–6061.
27 T. Sawano, N. C. Thacker, Z. Lin, A. R. McIsaac and W. Lin, *J. Am. Chem. Soc.*, 2015, **137**, 12241–12248.
28 A. H. Chughtai, N. Ahmad, H. A. Younus, A. Laypkov and F. Verpoort, *Chem. Soc. Rev.*, 2015, **44**, 6804–6849.
29 S. M. Cohen, *Chem. Rev.*, 2012, **112**, 970–1000.
30 N. T. S. Phan, K. K. A. Le and T. D. Phan, *Appl. Catal., A*, 2010, **382**, 246–253.
31 K.-I. Shimizu, K. Niimi and A. Satsuma, *Appl. Catal., A*, 2008, **349**, 1–5.
32 T. B. Poulsen and K. A. Jørgensen, *Chem. Rev.*, 2008, **108**, 2903–2915.
33 G. Dessole, R. P. Herrera and A. Ricci, *Synlett*, 2004, 2374–2378.
34 E. A. Hall, L. R. Redfern, M. H. Wang and K. A. Scheidt, *ACS Catal.*, 2016, **6**, 3248–3252.
35 A. Rostami, A. Colin, X. Y. Li, M. G. Chudzinski, A. J. Lough and M. S. Taylor, *J. Org. Chem.*, 2010, **75**, 3983–3992.
36 M. Bosch, M. Zhang and H.-C. Zhou, *Adv. Chem.*, 2014, **2014**, 1–8.
37 Z. Wei, W. Lu, H.-L. Jiang and H.-C. Zhou, *Inorg. Chem.*, 2013, **52**, 1164–1166.
38 K. S. W. Sing, D. H. Everett, R. A. W. Haul, L. Moscou, R. A. Pierotti, J. Rouquerol and T. Siemieniewska, *Pure Appl. Chem.*, 1985, **57**, 603–609.
39 X. Lin, J. Jia, X. Zhao, K. M. Thomas, A. J. Blake, G. S. Walker, N. R. Champness, P. Hubberstey and M. Schroder, *Angew. Chem., Int. Ed.*, 2006, **45**, 7358–7364.
40 W. Li, *Catal. Lett.*, 2014, **144**, 943–948.